Provided for non-commercial research and education use.
Not for reproduction, distribution or commercial use.

ISBN 978-90-481-9617-3

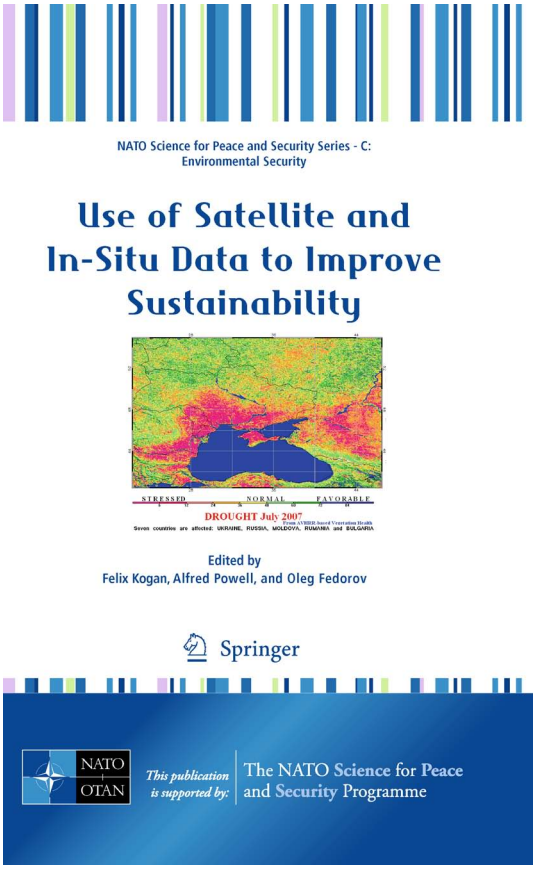


This chapter was published in the above Springer book. The attached copy is furnished to the author for non-commercial research and education use, including for instruction at the author's institution, sharing with colleagues and providing to institution administration.

Other uses, including reproduction and distribution, or selling or licensing copies, or posting to personal, institutional or third party websites are prohibited.

In most cases authors are permitted to post their version of the chapter (e.g. in Word or TEX form) to their personal website or institutional repository.

Author's personal copy

# Global Vegetation Health: Long-Term Data Records

**Felix Kogan, Wei Guo, and Aleksandar Jelenak**

**Abstract** The new Global Vegetation Health (GVH) data set has been developed for operational and scientific purposes. The GVH has advantages before other long-term global data sets, being the longest (30-year), having the highest spatial resolution (4-km), containing, in addition to NDVI, data and products from infrared channels, originally observed reflectance/emission values, no-noise indices, biophysical climatology and what is the most important, products used for monitoring the environment and socioeconomic activities. The processed data and products are ready to be used without additional processing for monitoring, assessments and predictions in agriculture, forestry, climate change and forcing, health, invasive species, deceases, ecosystem addressing such topics as food security, land cover land change, climate change, environmental security and others.

**Keywords** Vegetation health • 30-year 4-km data records • Vegetation Condition Index (VCI) • Temperature Condition Index (TCI) and Vegetation health indices (VHI) • NDVI and BT

## Introduction

One of the most important long-term (30 years) satellite-based data records characterizing land surface, air near the ground and climate were created from the Advanced Very High Resolution Radiometer (AVHRR) flown on the National Oceanic and Atmospheric Administration (NOAA) polar-orbiting satellites. Several

F. Kogan (✉)
NESDIS/NOAA, Center for Satellite Application and Research (STAR), Washington DC, USA
e-mail: felix.kogan@noaa.gov

W. Guo
IMSG Inc., Washington DC, USA

A. Jelenak
University Corporation for Atmospheric Research, Washington DC, USA

F. Kogan et al. (eds.), *Use of Satellite and In-Situ Data to Improve Sustainability*,
NATO Science for Peace and Security Series C: Environmental Security,
DOI 10.1007/978-90-481-9618-0_28, © Springer Science+Business Media B.V. 2011

Author's personal copy



global data sets were developed from the AVHRR records since the early 1980s. They were NOAA's Global Vegetation Index (GVI and GVI-2), NASA's Pathfinder and GIMMS (Tarpley et al. 1984; James and Kalluri 1994; Kidwell 1997; Tucker et al. 2004). These data were focused only on the Normalized Difference Vegetation Index (NDVI), ignoring infrared measurements, which are very useful for monitoring land, climate and socioeconomics. Therefore, NOAA has developed new data set entitled the Global Vegetation Health (GVH). The GVH has advantages before other long-term global data sets, being the longest (30-year), having the highest spatial resolution (4-km), containing, in addition to NDVI, data and products from infrared channels, originally observed reflectance and emission, many indices with suppressed noise, biophysical climatology and what is the most important, products used for monitoring the environmental and socioeconomic activities (Kogan 1995, 1997). This paper describes the new, considerably improved and currently available to users the NOAA's global AVHRR-based operational GVH data set at 4-km (0.036°) resolution.

## Satellites, Sensor, Data, Noise, Noise Removal, GVH Method

The 30-year, 4-km, 7-day composite GVH data records were developed from the measurements made by the AVHRR instrument flying on board NOAA polar-orbiting operational satellites. The NOAA/AVHRR is a cross-track scanning system (Kidwell 1995, 1997; Cracknell 1997) sensing the Earth and the atmosphere near the ground continuously through the 30-year history (from the early 1980s to the present) in the following wavelength of the solar spectrum: the visible (VIS, 0.58–0.68 μm, channel 1 (Ch1)), near infrared (NIR, 0.725–1.1 μm, channel 2 (Ch2)) and two infrared (IR, 10.3–11.3 μm, channel 4 (Ch4) and 11.5–12.5 μm, channel 5 (Ch5)). The AVHRR instrument scans the Earth continuously at a 1.1-km ground resolution and the measurements are sampled and recorded for the entire globe at 4-km resolution contributing continuously to the NOAA's Global Area Coverage (GAC) data set (Cracknell 1997).

From the 14 NOAA satellites flying in sun-sinchronous orbit and carrying the AVHRR instruments, the GVH system and data sets were developed from seven afternoon satellites: NOAA-7, 9, 11, 14, 16, 18 and 19 launched on June 23, 1981 (local day time at launch 14:30), December 12, 1984 (14:20), September 24, 1988 (13:30), December 30, 1994 (13:30), September 21, 2000 (13:44), May 20, 2005 (13:50) and June 2, 2009 (13:44), respectively. These satellites operated during 1981–1985, 1986–1989, 1989–1994, 1995–2000, 2001–2005, 2005 to present and 2009 to present, respectively. During September 1994–January 1995 no afternoon operational observations were produced since NOAA-11 satellite was malfunctioned and new NOAA-13 satellite failed soon after launch. Also, during January–June 2005, NOAA-16 was malfunctioning from time to time and its data were replaced with NOAA-17 (morning satellite) preliminary calibrated to the

Author's personal copy



NOAA-16 data. From the indicated satellites, NOAA-7 and 9 carried AVHRR-1 instrument, NOAA-11 and 14 – AVHRR-2 and the rest – AVHRR-3. All of them have identical design but with slightly different response functions.

The VIS and NIR channels were pre-launch calibrated for converting counts into reflectance. The IR channels were in-flight calibrated and their count values were converted to brightness temperature. Due to chlorophyll and carotenoid pigments, leaf interior (mesophyll structure) and water content in green vegetation, the VIS and NIR measurements provide a means of monitoring vegetated surfaces. Difference between the NIR and VIS increases when vegetation becomes greener, more vigorous (more water) and denser. This is the main principle for the vegetation indices. The (NIR-VIS) difference was normalize representing the Normalized Difference Vegetation Index (NDVI = (NIR − VIS)/(VIS + NIR)). The IR channels were corrected for non-linear behavior of the instrument (Cracknell 1997).

The GVH system algorithm starts form data extraction from the AVHRR/CLAVR-x processing system (Jacobowitz et al. 2003; Heidinger and Pavolonis 2009) and collating the data onto a global GVH grid. This grid is based on the Plate Carre map projection. The global data spans from 75.024° (north edge) to −55.152° (south edge) in the latitudinal and from −180° (west) to 180° (east) in longitude directions. This processing supports nominal grid cell length of 4-km (3,616 * 10,000 grid elements).

The GVH input includes the CLAVR-x navigation (NAV), observation (OBS), and geo-location (GEO) files for each Global Area Coverage (GAC) Level 1b orbit. Daily data are aggregated to a 7-day period using compositing method (saving the day which has the highest NDVI during the period). The compositing starts on the first day of a year and a period must have at least 4 days in the same year. The GVH output is a single file for each processing period containing metadata for each output variable, sensor and solar zenith angle, relative azimuth angle and ch1, ch2 counts and ch4, ch5 brightness temperature in the Hierarchical Data Format (HDF) similar to CLAVR-x output.

One of the important steps in the primary data processing is radiometric calibration of visible and correction of thermal channels. Visible channels' calibration consists of generally two steps: pre- and post-launch calibration. Based on Kidwell (1995), the following pre-launch linear formula ($A = S * C + I$) is applied, where ($A$) is albedo, ($S$) is slope and ($I$) is intercept. Since the instrument output does not remain the same after launch, post-launch calibration was applied ($R = S * (C - cd)$) to NOAA-7 to 14 satellites, where $C$ is 10-bit radiance count and $cd$ – dark count) following Rao and Chen (1993, 1999). For NOAA-16 through 19 a dual slop calibration method was applied.

*Long- and Short-term Noise.* Noise in AVHRR data creates fundamental constraints to the remote sensing of the Earth. The noise sources are physical, geometrical, mechanical, mapping, environmental, random etc.; some of them long-term, some short-term and some both (Kogan et al. 1996; Rao and Chen 1993, 1999; Cracknell 1997; Kidwell 1997). Clouds and other atmosphere constituents (aerosol, water vapor etc.) obscure the land surface reducing NDVI considerably. In case of unusual events, such as sharp volcanic aerosol increase, NDVI can be

Author's personal copy



depressed for a long time (Kogan et al. 1994). Changes in viewing and illumination geometry can lead to both an increase and decrease in NDVI depending on location, type of vegetation, position of sun and sensor. Satellite orbital drift, sensor degradation, and satellite change create long-term noise in NDVI data, especially after a satellite has been in service for more than 3 years.

A few techniques have been designed to detect and reduce some noise in AVHRR data such as cloud and aerosol-screening, bi-directional effects, pre- and post-launch calibration, geometry effects, sensor degradation satellite orbital drift. Regardless of all these achievements, a complete physically based correction for all effects over various land surfaces, able to eliminate high, medium and low frequency noise, is not available. Unfortunately, NDVI and IR annual time series values experience large fluctuations (Kogan 1995) introducing some errors when this data is used for monitoring purposes. Many of these fluctuations are associated with non-physical causes, such as method of data sampling and processing, satellite navigation and orientation, observation and communication errors, and other random noise. It is unlikely to develop corrections for this type of noise. Besides, if clouds are detected the data are discarded, leaving a hole on a map. This put additional constraint on AVHRR data utility.

In the development of GVH method and algorithm, major long- and short-term noise creating problem for satellite data interpretation and applications was removed from the data. They are (a) satellite orbit and sensor degradation; (b) jumps between the satellites; (c) excessive stratospheric aerosols; (d) difference in Equator crossing time; (e) difference between AVHRR sensors; (f) high frequency (short-term) noise; (g) random noise. Some of the noise sources are interrelated, some have additive impact, some has either short- or long-term contribution and some provides a combine input. Visible channels are affected by all noise sources, while infrared mostly by short-term because they are calibrated on board.

A large satellite data distortion in the visible channels and NDVI occurs due to such long-term noise as satellite orbital drift, AVHRR sensor degradation and excessive stratospheric aerosols from volcanoes. The orbital drift and sensor degradation affected visible measurements on all space platforms; they normally start 2–3 years after a satellite was in space. NDVI reduction was observed on the data collected from NOAA-9 during 1987 and 1988, NOAA-11 (1993 and 1994) and NOAA-14 (1999 and 2000). In addition, reflectance/emission measured from NOAA-11 were distorted due to elevated stratospheric aerosols during 1991–1993 resulted in NDVI reduction. The aerosol was built after eruption of Mt Pinatubo volcanoes in the Philippines in mid-June 1991. In a few weeks after eruption, the aerosols encircled the Earth with the major air flow and stayed in the area between 30–20°N and 20–25°S for nearly 1.5–2 years. As the result the NDVI in that area dropped almost in half during second part of 1991 through 1992 (Kogan et al. 1996; Vargas et al. 2009). Similarly, NDVI reduced in tropical latitudes in April 1982 for 1–2 years after eruption of El Chichon volcano in Mexico (Stowe et al. 1992).

Some difference between NDVI calculated from NOAA-16 and 18 satellites reflectance and from NOAA-14 and 11 existed during 2000–2010. This occurred because the AVHRR-3 instrument has slightly different characteristics than

Author's personal copy



AVHRR-2. Specifically, the area under response function curve for the first two was 8–12% narrower than for the last two. As the result the NDVI from NOAA-16 and 18 turned out to be higher than for the previous satellites. Moreover, in addition to NDVI reduction for NOAA-7 and 9 due to stratospheric aerosol and sever orbit degradation, general level of NDVI for the 1981–1988 period was 10–15% smaller than for the next two satellites because the time of the equator crossing for the first two satellites was almost one hour later. As the result of these problems and also orbit-degradation errors, large jumps in NDVI were observed between the end of previous and the beginning of the next satellites. The IR channels are also affected by stratospheric aerosol and orbit degradation (although less than the VIS) and must be corrected.

Finally, high frequency noise inside each year created by clouds, variable transparency of the atmosphere (water vapor, dust, chemicals etc.), surface anisotropy, geometry of the sun and sensor, position of satellite, methods of data processing, random noise (including human errors) and long-term sources of noise distort considerably reflectance/emission of both NDVI and BT creating difficulties for satellite data application.

*Noise removal.* As it has been mentioned, quite often different sources of noise affect NDVI and BT: either reducing their values (sensor degradation, orbital drift, equator crossing time, atmospheric attenuation, volcanic eruptions etc.) or increasing (spectral response function, off-nadir view etc.) or both depending on parameters (sensor type, surface anisotropy, forward/backscattering, sampling, random errors etc.). Moreover, quite often, several sources of noise affect the measured parameters the same time and with different intensity. It is hard to develop individual procedure for each source of noise because it is unknown how to separate them (for example elevated stratospheric aerosol and sensor/orbit degradation). Therefore, the noise in GVH data was removed empirically by comparing satellite and in situ observations applying the methods of mathematical statistics plus validation.

Bias related to sensor degradation, satellite orbital drift, jumps in the indices while transitioning from one satellite to the next/previous and an elevated stratospheric aerosol were removed by applying the Empirical Distribution Function (EDF) method. (Crosby et al. 1996). An EDF is based on the assumption that for large areas, the NDVI reduction due to technical and external forces (orbital drift, volcanic eruptions, etc.) is larger than the weather-related NDVI changes from year to year. This can be expressed through probability that a random variable $X$ is less than a given value $x$ [$F(x) = Pr\{X < x\}$]. Following this assumption, large and stable changes in NDVI and BT can signal unexpected disturbances due to non-weather related causes discussed here. As a rule, sensor and satellite orbital degradation, increase and aerosol reduce NDVI and BT. This negative effect can be reduced by adjusting the EDF of parameters for the affected years with a benchmark EDF for the non-affected. The benchmark EDF for NDVI and BT were statistically composited from data of the 5 non-affected years: 1989, 1990, 1995, 1996, and 1997 (Vargas et al. 2009). The benchmark EDF's for NDVI and BT were developed for each latitude lines and week of the year. The normalization of

Author's personal copy



the distorted data was performed for each pixel inside every latitude line and for each week by adding the difference between distorted and benchmark EDFs to each distorted pixel values of NDVI and BT for each latitude line and week. The thresholds (0.01 for NDVI and 2°C for BT) for the correction was selected based on data analysis.

A stable long-term bias between NDVI from NOAA-16, 18 (2000–2010) and previous satellites due to response function differences was removed by calibrating the distorted NDVI against the NDVI measured by an on-ground radiometer during the growing season of 2002 over soybeans and corn at the experimental station of the University of Nebraska-Lincoln. During that period the fields' vegetation fraction (VF) changed from 10 at the beginning of the season to 90% at the end. The in situ NDVI were compared with the top-of-canopy NDVI (obtained by running radiative transfer model) from AVHRR-3 sensor on NOAA-16. The comparison showed that NOAA-16 and later NOAA-18 NDVI must be reduced by 10% for all VF in order to remove response function curve differences with previous satellites.

Another stable long-term bias, lower NDVI level for NOAA-7 and 9 (1981–1989) compared to the later satellites, was investigated. A half an hour data collected from the Spinning Enhanced Visible and Infrared Imager (SEVIRI) on the Meteosat Second Generation (MSG-2) European satellites were used to investigate NDVI dynamics in relation to the local time of observations. The results indicated that the bias developed because for the earlier satellites the equator crossing time was half to one and a half hours later than for the following satellites. SEVIRI's NDVI analysis for the 2009 indicated that NDVI drops between 6% and 11% if observation local time moves from 13:00 to 14:30. In order to correct this distortion the EDF method was used.

High frequency noise (clouds, aerosol, bi-directional reflectance, sun and sensor angles, human errors, other random noise) were removed from NDVI and BT by applying statistical methods. The vegetation-oriented method for a comprehensive noise reduction stems from a statistical approximation of the vegetation and temperature annual time series. The idea was to (a) single out the seasonal cycle; (b) suppress high frequency noise, and (c) enhance medium and low frequency variations related to large-scale and persistent weather fluctuations. This technique considers smoothing the weekly time series with a combination of a compound median filter and the least squares technique (Kogan et al. 1997). Numerous tests showed that this smoothing eliminated completely the high frequency outliers, including random, approximated accurately the annual NDVI and BT cycles, and, more importantly, singled out medium-to-low frequency weather-related fluctuations (valleys and hills in the NDVI and BT time series) during the annual cycle (Kogan 1995).

Figure 1 shows time series of completely processed no noise NDVI averaged over three 1.0° latitudinal circles. Each diagram covers several ecosystems: broadleaf forest (54.5–55°N), mostly desert with some contribution from Southeast Asia forest (24.5–25°N) and mostly tropical forest (5.0–5.5°S). As seen, the time series (a) after do not show neither long-term trend nor short-period (5–10 years) trends;

Author's personal copy



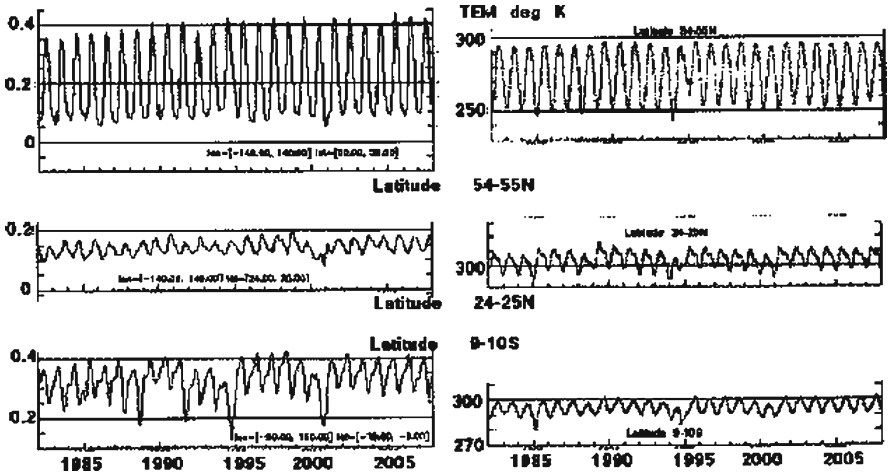


**Fig. 1** Processed mean NDVI (*left*) and BT (*right*) for three global latitude bands

(b) there are no any jumps between the satellites (1985–1986, 1988–1989, 1994–1995); (c) no NDVI reduction due to satellite orbit, sensor degradation and excessive stratospheric aerosols (1982–1984 and 1991–1994); (d) no difference due to Equator crossing time; (e) no difference due to AVHRR sensors changes; and (f) no high frequency and random noise are observed.

*GVH Method.* After noise removal, weather-driven differences in NDVI and BT between the years become apparent: lower NDVI and higher BT in dry years and opposite in normal and wet years. This principle of comparing NDVI and BT for a particular year with their dry–wet range calculated from 30-year observations was laid down in the GVH algorithm development. The absolute maximum and minimum of NDVI and BT during 1981–2005 were calculated for each of the 52 weeks and for each pixel. They were then used as the criteria to estimate the upper (favorable weather) and the lower (unfavorable weather) limits of the ecosystem resources. Further, for estimation of weather impacts on vegetation condition, NDVI and BT values for a particular time (1 week or several weeks) were normalized relative to the absolute max/min interval. Following this procedure, NDVI and BT were rescaled based on Eqs. (1–3). They were named the Vegetation Condition Index (VCI), Temperature Condition Indices (TCI) and Vegetation Health Index (VHI) designed to characterize moisture (VCI), thermal (TCI) and total vegetation health (VHI) conditions in response to weather impacts

$$\mathrm{VCI} = 100 * (\mathrm{NDVI} - \mathrm{NDVI}_{\min}) / (\mathrm{NDVI}_{\max} - \mathrm{NDVI}_{\min}) \tag{1}$$

$$\mathrm{TCI} = 100 * (\mathrm{BT}_{\max} - \mathrm{BT}) / (\mathrm{BT}_{\max} - \mathrm{BT}_{\min}) \tag{2}$$

$$\mathrm{VHI} = a * \mathrm{VCI} + (1 - a) * \mathrm{TCI} \tag{3}$$

Author's personal copy



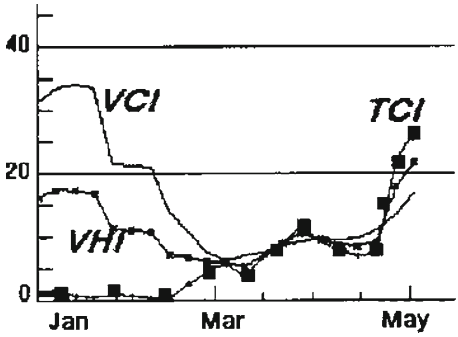


**Fig. 2** Dynamics of vegetation health indices during the 2009 spring drought in southern Taxes (for a box with longitude 98.0–97.7°W, latitude 28.0–28.3°N) from NOAA-18 satellite

where NDVI, NDVImax, and NDVImin (BT, BTmax, and BTmin) are the smoothed weekly NDVI (BT), their multi-year absolute maximum, and minimum, respectively. The VCI, TCI and VHI approximate the weather component in NDVI, BT and their combination values. They fluctuate from 0 to 100, reflecting changes in vegetation conditions from extremely bad to optimal.

An example of VH assessment and analysis of the 2009 spring drought in the southern Taxes is shown in Fig. 2. As seen, all indices show drought (below 40) from January 2009. The worse conditions developed due to extremely high temperatures (TCI close to 0), which continued through the entire spring (almost 4 months). As the result of the extreme heat, VCI (moisture index), which indicated mild (30–40) drought in January start deteriorated quickly reaching extreme drought level of 5–10 during March and April. Since both VCI and TCI showed extreme drought conditions the total vegetation health conditions were extremely unfavorable. In May, drought recovery has started, because the temperature cooled off.

## Conclusions

The new Global Vegetation Health (GVH) data set has been developed for operational and scientific purposes. The GVH has advantages before other long-term global data sets, being the longest (30-year), having the highest spatial resolution (4-km), containing, in addition to NDVI, data and products from infrared channels, originally observed reflectance/emission values, no-noise indices, biophysical climatology and what is the most important, products used for monitoring the environment and socioeconomic activities. The processed data and products are ready to use without additional processing, since the noise was completely removed and the products were developed based on vegetation requirements and the laws governing the vegetation. In addition to monitoring, the GVH data can be used for predictions since some parameters such as NDVI, VCI and partially VHI have "memory" reflecting cumulative impacts of the environment on vegetation canopy (Kogan 1995). GVH time series can be also used for climate-related trend analysis

Author's personal copy



such as vegetation green up, start/end of the growing season, gross primary production, losses in vegetation productivity, land cover change etc. It is important also to mention a few data correction procedures ignored in other global data. A few of them are removal of high frequency noise, also difference in response functions between AVHRR-3 and previous versions of the instruments, inconsistencies between the satellites in equator crossing time parameter. Moreover, some corrections were verified versus in situ data to see if the data quality is improving. The next steps in this research is comparison of GVH with other global datasets and analysis of climate induced vegetation green up.

## References

Cracknell AP (1997) The advanced very high resolution radiometer. Taylor & Francis, USA, 534 p

Crosby DS, Goldberg MD, and Chung W (1996) Inter-satellite calibration using empirical distribution functions. 8th Conference on Satellite Meteorology and Ocean, Atlanta GA. American Meteorological Society, pp 188–190

Heidinger AK, Pavolonis MJ (2009) Global daytime distribution of overlapping cirrus cloud from NOAA's Advanced Very High Resolution Radiometer. J Climate 18(22):4772–4784

Jacobowitz H, Stow LL, Ohring G, Heidinger A, Knapp K, Nalli N (2003) The advanced very high resolution radiometer PATHFINDER Atmosphere (PATMOS) climate data set: a resource for climate research. Bull Am Meteorol Soc June:785–793

James ME, Kalluri SN (1994) The Pathfinder AVHRR land data set: an improved coarse resolution data set for terrestrial monitoring. Int J Remote Sensing 15:3347–3363

Kidwell KB (ed) (1997) Global vegetation index user's guide. National Oceanic and Atmospheric Administration, National Environmental Satellite Data and Information Services, National Climatic Data Center, Camp Springs MD, USA

Kidwell KB (ed) (1995) NOAA polar orbiter data users guide. National Oceanic and Atmospheric Administration, National Environmental Satellite Data and Information Services, National Climatic Data Center, Camp Springs MD, USA

Kogan FN (1997) Global drought watch from space. Bull Am Meteorol Soc 78:621–636

Kogan FN, Sullivan JT, Ciren PB (1996) Testing post-launch calibration for the AVHRR sensor on world desert targets during 1985–1993. Adv Space Res 17(1):47–50

Kogan FN (1995) Droughts of the late 1980s in the United States as derived from NOAA Polar Orbiting Satellite Data. Bull Am Meteorol Soc 76:655–668

Kogan FN, Sullivan J, Carey R, Tarpley D (1994) Post-pinatubo vegetation index in Central Africa. Geocarto Int 3:51–58

Rao CRN, Chen J (1993) Calibration of the visible and near-infrared channels of the Advanced Very High Resolution Radiometer (AVHRR) after launch. Proceedings the International Society of Optical Engineering, Orlando, FL, pp 56–66

Rao CRN, Chen J (1999) Revised post-launch calibration of the visible and near-infrared channels of the Advanced Very High Resolution Radiometer on the NOAA-14 spacecraft. Int J Remote Sensing 20:3485

Stowe LL, Carey RM, and Pellegrino PP (1992), Monitoring the Mt.Pinatubo aerosol layer with NOAA/11 AVHRR data, Geophys. Res. Lett., 19:159–162.

Tarpley JP, Schneider SR, Money RL (1984) Global vegetation index from NOAA-7 meteorological satellite. J Climate Appl Meteorol 23:491–494

Vargas M, Kogan F, Guo W (2009) Empirical normalization for the effect of volcanic stratospheric aerosols on AVHRR NDVI. Geophys Res Lett 36:L07701

Tucker CJ, Pinzon JE, Brown MB, Slayback DA, Pak EW, Mahoney R, VermoteEF, El Salcous N (2004) An extanded AVHRR 8-km NDVI data set compatible with MODIS and SPOT vegetation NDVI data. Int J Remote Sensing 15(7):340–354